



DEPOSITIONAL ENVIRONMENTS, TEXTURAL AND MINERALOGICAL CHARACTERISTICS OF THE EXPOSED QUATERNARY SEDIMENTS, GIZA, EGYPT

El Sayed, O.¹, Mahmoud, A. A.¹, Gad, A.², Khattab, A.¹

1 Department of Biological and Geological Sciences, Faculty of Education, Ain Shams University, Cairo
2 Geology Department, Faculty of Science, Ain Shams University, Cairo, Egypt

ABSTRACT

Quaternary sediments are extensively exposed in Kafr El Gebel area, south of Sphinx, Giza, Egypt. Ten stratigraphic sections have been chosen for studying and sampling. Fifty one samples were collected to investigate sedimentological and mineralogical characteristics of the Quaternary sediments. The statistical grain size parameters revealed that the investigated sands are mainly medium to coarse, very well sorted to poorly sorted, mostly near symmetrical skewed accompanied by mesokurtic to leptokurtic characters. The textural characteristics strongly suggest that fluvial conditions of braided river were most probably the dominating factors controlling the transportation and accumulation of the investigated sediments. The light minerals of the investigated sand are composed mainly of quartz with minor amount of feldspars. The non-opaque heavy mineral assemblages of the Quaternary sediments are characterized by the predominance of pyroxene, amphiboles, epidote, zircon, tourmaline, rutile, garnet, staurolite and kyanite. Andalusite, titanite and monazite are recorded in a few samples. The low values of ZTR index suggesting mineralogically immature nature of these sediments. The heavy minerals assemblage of these sediments assemblage indicates a variety of probable source rock types including metamorphic, igneous, and sedimentary.

Keywords: Grain size, Heavy minerals, Geochemical, Quaternary sediments, Giza

INTRODUCTION

It is well known that, generating and sedimentation of detrital materials are controlled by a different varieties including the lithology and composition of the source rock, relief and climatic condition in the source area, as well as sediment transport and sedimentation mechanisms (e.g. Johnsson, 1993; Abuodha, 2003; Weltje and von Eynatten, 2004; von Eynatten and Dunkl, 2012). Systemic presentation and analysis of textural, mineralogical composition and geochemistry of detrital sediments data provide evidence of the composition of the source rocks, weathering processes and transport history (Friedman, 1961; Folk, 1966; Lario et al., 2002; Garzanti et al., 2009; Alharbi et al., 2016). Clarification of these data aids in disentangle of depositional environment and elucidate transporting medium nature and dynamics (Mycielska-Dowgiało and Ludwikowska- Kędzia, 2011). Mineralogical composition of unconsolidated and consolidated detrital sediment, especially the properties of heavy minerals (HM) assemblage have long been regarded as sensitive indicators of sediments sources and permit their extensive use in tracing provenance (Nechaev and Ispording, 1993; Morton and Hallsworth, 1994; Wong, 2002; Kasper-Zubillaga et al., 2008; Giorgetti et al., 2009; Sawakuchi et al., 2009; Lahijani and Tavakoli, 2012; Garzanti et al., 2019). The principal factors controlling HM assemblages in detrital sediments are source rock mineralogical composition, mineral size and shape, specific gravity and stability during transportation, weathering and diagenesis. Chemical weathering during fluvial transport reduces the heavy mineral diversity (Johansson and Meade, 1990; Savage and Potter 1991; Garzanti et al., 2019).

The River Nile and its annual floods have delivered detrital sediments from diverse regions that differ from each other in geomorphology, bedrock geology, climatic zones, and soils to the floodplain of Egypt for millennia (Foucault and Stanley, 1989; Said, 1993). The oldest delta of The River Nile is preserved and recorded near Fayoum and have been dated as Eocene (38–35 Ma) (Salem, 1976; Underwood et al., 2013). The delta began to pro-grade north as the Tethys Ocean receded, depositing in its current offshore

location from the Oligocene (30 Ma) (Craig et al., 2011). Sediment accumulation continued in the Mediterranean until the end-Miocene Messinian Salinity Crisis (Dolson et al., 2001), after which the Zanclean flood rapidly filled the Mediterranean basin. An increase in sedimentation rate in the Nile delta cone during the Late Pliocene–Early Pleistocene is proposed by Macgregor (2012) to result from uplift of the Ethiopian Rift shoulders, with associated increased rainfall and erosion.

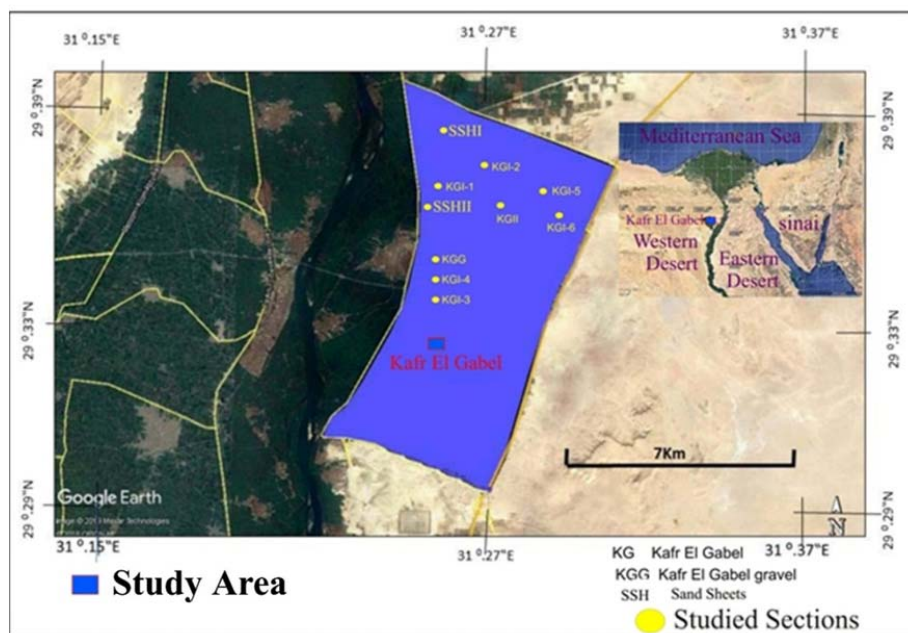
Study of alluvial sediments in the Nile Valley and Delta has a long history, starting at the beginning of 20th Century. Most of these studies were focused on the Pleistocene Nile sediments in Upper Egypt (e.g. de Heinzelin, 1968; Butzer and Hansen, 1968; Said, 1981, 1993). Also, Holocene Nile floodplain sediments were subjected to intensive archaeological and geological investigations (e.g. Wendorf and Schild, 1976). Investigations into the mineralogy of the Nile sediments began with the pioneering work of Shukri (1950), which led to plentiful heavy-mineral studies on River Nile sediments in Egypt (e.g., Hassan, 1976; Foucault and Stanley, 1989; Frihy et al. 1995; Garzanti et al., 2006, 2015, 2019). A few studies were also carried out on clay minerals and geochemistry of Nile sediments (e.g. Stanley and Wingerath, 1996; Siegel et al., 1995; Dawood and Abd El Naby, 2012; Fielding et al., 2018; Hamdan et al., 2019).

The aim of the present work is two-fold: (i) to investigate the detailed textural and mineral characteristics of the Quaternary sediments in Kafr El Gabal area; (ii) to elucidate the sedimentary history of these sediments.

STUDY AREA

The Study area "Kafr El Gebel" is located near the large delta of the Nile River on the west bank of the River Nile, opposite the modern Egyptian capital of Cairo, 17 kilometres to the north of Saqqara and some 8 kilometres to the south of Abu Rawash, south of the Sphinx by 19 km. It's bounded by Longitudes 31° 15' -31° 37' E and Latitude 29° 29' - 29° 39' N (Fig. 1).

Fig. 1: Location Map of the study area.



GEOLOGIC SETTING

The rock forming the Giza Pyramids Plateau consists mainly of white, yellow argillaceous and dark gray dolomitic limestone representing the Middle Eocene (Omara, 1952) (Fig. 2). These rocks are interbedded with thin layers of argillaceous limestone in their upper part. These Middle Eocene rocks are made up of two distinct units, called the Mokattam and the Observatory formations. These formations are exposed at the edge of the plateau and are overlaid by the Maadi Group (Strougo, 1985). The Maadi Group is subdivided into three units, these are from older to younger; the Qarn Formation, the Wadi

Depositional environments, textural and mineralogical characteristics

Garawi Formation and the Wadi Hof Formation. The top unit of the Maadi Formation comprises several meters of massive, partly dolomitized limestones (pack—grainstones) of the so-called "Ain Musa Bed" (Strougo, 1979). The Maadi Formation shows a gentler escarpment toward the Mokattam Formation in the north and to the Nile valley alluvium in the east.

Post Eocene rocks are represented by Pliocene deposits. They are found in the southern part of the study area and consist of two units. The older one is the Kom el Shellul Formation which consists of fossiliferous marine sandstone; and the younger one called the Helwan Formation (Said, 1975), which consists of laminated fluvial gray shale and siltstone.

The plains and the different wadis of the different hills of the Giza Pyramids Plateau are covered by an alluvium formed of polymictic sands and gravels, the probable age of each is Pleistocene and Recent (Mahmoud and Hamdan, 2002). These sediments are subdivided into three units which called from older to younger as follows, the Kasr El Basil Formation (cross-bedded, gravel and coarse- to medium grained quartzose sand), the Abbassia Formation (yellowish brown quartzose sand and light gray cross laminated pebbly coarse- to medium grained sand), the Kafr El Gebel Formation (brownish yellow loose pebbly coarse- to medium and fine- to medium grained quartzose sand) (Mahmoud and Hamdan, 2002).

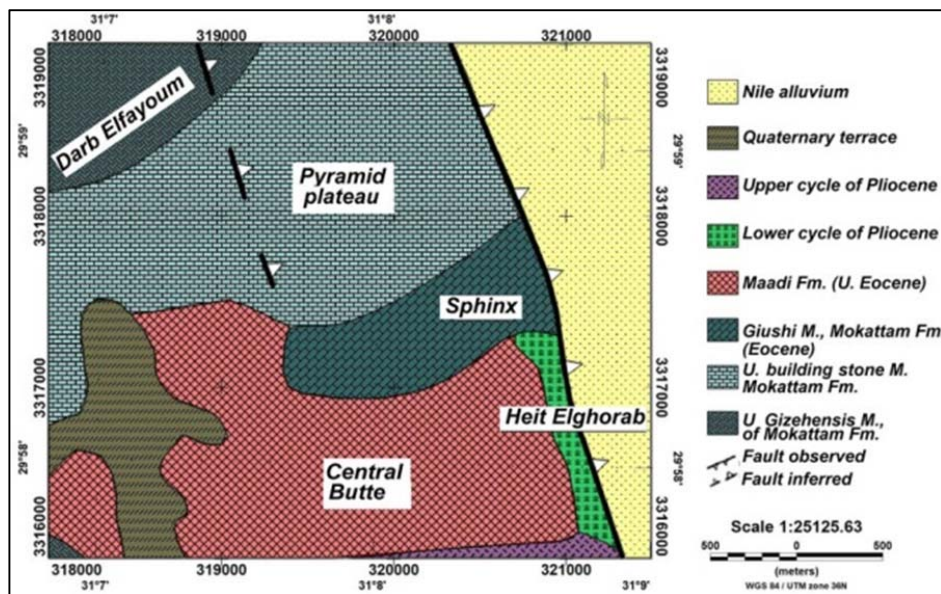


Fig. 2: Geologic map of the Giza Pyramid Plateau, Egypt (Sharafeldin et al. 2019).

SAMPLING AND ANALYTICAL PROCEDURES

Ten stratigraphic sections were carefully measured, described and sampled (Fig. 1). A total of forty nine samples were collected from the study area representing Late Pleistocene (15 sample), Middle Pleistocene (22 sample), Early Pleistocene (3 samples) and Holocene (9 samples). In addition, eighty six grains of gravel size were collected (Early Pleistocene).

For grain-size-distribution analysis, dry sieving technique was conducted. 100 g of each sample were sieved using a Ro-Tap shaking machine for 20 m, with - 1, 0, 1, 2, 3, and 4 Ø set of standard mesh sieves. The textural parameters according to Folk and Ward (1957) were calculated with phi values Ø 5, Ø 16, Ø 25, Ø 50, Ø 75, Ø 84, and Ø 95, obtained from the cumulative curves. The collected rock gravels are studied according to their sphericity, shape and size.

Mineralogically, representative bulk samples were analyzed by XRD using a PANalytical X-Ray Diffraction equipment model X'Pert PRO with monochromator, Cu-radiation ($\lambda=1.542 \text{ \AA}$) at 40 Kv, 40 mA and scanning speed $0.03^\circ/\text{sec}$. Heavy minerals have been separated from 63–125 μm and 125–250 μm (fine and very fine sand-size fractions) by standard technique (Galehouse, 1971; Mange and Maurer, 1992) using bromoform (specific gravity 2.85) as the heavy liquid. Separated heavy fraction was washed with acetone and ethyl alcohol and then mounted on glass slide with Canada balsam. More than 300 grains per sample have been counted in each heavy mineral mount. The heavy and light minerals were identified





under Olympus polarized microscope (Mange and Maurer, 1992). The mineralogical composition was calculated in grain percentages. ZTR index (percentage of Zircon-Tourmaline-Rutile/Non-Opauques) was calculated following Hubert (1962). The thin sections of the collected gravels were examined by Olympus Polarized microscope.

RESULTS AND DISCUSSIONS

Lithofacies

The main field observations are summarized and presented in Table 1. The Pleistocene (pre-Nile) deposits of the pyramid plateau area include gravels, channel-bar sands; laminated inter-mud clast conglomerates overlay an erosion surface. The channel-bar sediments characterized by the presence of small and medium planar and trough cross bedding (Mahmoud and Hamdan, 2002; Mahmoud, 2018). These sedimentary features indicate that the depositional environment might be braided river.

Table 1: Types of the lithofacies of the studied exposed Quaternary Sediments.

Age	Lithofacies	Interpretation	
The Holocene	Sand sheets	Loose, medium grain size, poorly sorted, humic materials sand sheets.	
Late Pleistocene	Wedged shape cross bedding sand	Wedged shape, cross bedding, moderately sorted, these units are channel bar sediments.	
Middle Pleistocene	Large scale cross bedding sand	Hard cross bedded medium to coarse sand, moderately sorted, these units are channel bar sediments.	
Early Pleistocene	Gravelly sand	Gravelly sand, loose, moderately sorting, high and vigerous fluvial energy currents.	

Grain-size analysis

Grain-size distributions of the studied sediments samples and their parameters calculated using Folk and Ward's (1957) formula are given in Table 2 and Table 3. The obtained grain size data are plotted on the gravel, sand, and mud ternary diagram (Fig. 3) (Folk, 1954). The sand fraction is the most common grain size in the studied sediments samples. The data revealed that the Early Pleistocene sediments are

Depositional environments, textural and mineralogical characteristics

classified as 93.33 % sand and 6.67 % gravelly sand. The Middle Pleistocene sediments are classified as 63.64 % sand, 13.64 % gravelly sand and 22.72 % sandy gravel. The Late Pleistocene sediments are classified as 66.67 % sand and 33.33 % gravelly sand. On the other hand, the Holocene sediments are classified as 88.89 % sand and 11.11 % gravelly sand. Moreover, the Pleistocene sediments are generally coarser than Holocene sediments.

Table 2 Percentages of different size fractions and their textural nomenclature of the studied sediments

Age	S. No.	Gravel %	Sand %	Mud %	Nomenclature (Folk, 1954)
Early Pleistocene	1	7.46	92.31	0.23	Sand
	2	21.17	78.36	0.47	Gravelly Sand
	3	7.23	92.52	0.24	Sand
	4	4.35	94.57	1.08	Sand
	5	2.60	95.73	1.67	Sand
	6	2.89	94.82	2.29	Sand
	7	0.56	94.41	5.04	Sand
	8	1.05	96.99	1.96	Sand
	9	0.07	96.97	2.96	Sand
	10	1.01	94.62	4.38	Sand
	11	3.05	95.00	1.95	Sand
	12	3.13	93.98	2.88	Sand
	13	2.17	97.30	0.53	Sand
	14	2.97	96.44	0.60	Sand
	15	5.39	94.22	0.40	Sand
Middle Pleistocene	16	9.71	87.12	3.17	Gravelly Sand
	17	5.33	94.37	0.31	Sand
	18	51.02	47.98	1.00	Sandy Gravel
	19	1.99	97.62	0.40	Sand
	20	0.14	99.39	0.47	Sand
	21	1.84	97.89	0.27	Sand
	22	2.70	97.04	0.25	Sand
	23	7.47	92.39	0.14	Sand
	24	25.52	73.99	0.49	Gravelly Sand
	25	1.80	98.03	0.17	Sand
	26	3.45	96.49	0.06	Sand
	27	0.38	98.73	0.89	Sand
	28	53.52	45.04	1.45	Sandy Gravel
	29	12.26	87.57	0.17	Gravelly Sand
	30	1.20	98.62	0.18	Sand
	31	8.51	91.07	0.42	Sand
	32	54.25	45.57	0.18	Sandy Gravel
	33	39.65	59.90	0.44	Sandy Gravel
	34	46.52	53.18	0.30	Sandy Gravel
	35	0.39	99.20	0.41	Sand
	36	4.05	95.46	0.49	Sand
	37	0.35	99.41	0.24	Sand
Late Pleistocene	38	11.99	87.32	0.70	Gravelly Sand
	39	0.06	99.60	0.34	Sand
	40	4.18	95.51	0.30	Sand
Holocene	41	4.59	95.04	0.37	Sand
	42	3.88	95.52	0.60	Sand
	43	5.51	94.13	0.36	Sand
	44	3.21	95.66	1.13	Sand
	45	5.28	93.06	1.66	Sand
	46	3.99	94.72	1.29	Sand
	47	1.92	92.31	5.77	Sand
	48	2.87	96.59	0.54	Sand
	49	24.36	74.87	0.77	Gravelly Sand

Table 3 Grain size parameters of the studied sediments samples

Age	S. No.	Mean size (Mz)	Standard deviation (σ)	Skewness (SK)	Kurtosis (KG)				
Early Pleistocene	1	0.37	Coarse Sand	0.28	V well sorted	-0.05	Nearly symmetrical	1.01	Mesokurtic
	2	0.17	Coarse Sand	0.21	V well sorted	0.06	Nearly symmetrical	0.66	Very platykurtic
	3	0.40	Coarse Sand	0.37	Well sorted	0.05	Nearly symmetrical	0.91	Mesokurtic
	4	0.63	Coarse Sand	0.55	Moderately well sorted	0.07	Nearly symmetrical	0.85	Platykurtic
	5	1.27	Medium Sand	0.93	Moderately sorted	-0.20	Coarse skewed	1.39	Leptokurtic
	6	1.30	Medium Sand	0.97	Moderately sorted	-0.15	Coarse skewed	1.30	Leptokurtic
	7	1.70	Medium Sand	1.47	Poorly sorted	0.09	Nearly symmetrical	1.52	Very leptokurtic
	8	1.37	Medium Sand	1.08	Poorly sorted	-0.04	Nearly symmetrical	1.35	Leptokurtic
	9	1.77	Medium Sand	1.46	Poorly sorted	0.12	Fine Skewed	1.32	Leptokurtic
	10	1.73	Medium Sand	1.44	Poorly sorted	0.07	Nearly symmetrical	1.60	Very leptokurtic
	11	1.50	Medium Sand	1.12	Poorly sorted	-0.14	Coarse skewed	1.09	Mesokurtic
	12	1.27	Medium Sand	1.01	Poorly sorted	-0.10	Nearly symmetrical	1.29	Leptokurtic
	13	1.23	Medium Sand	0.95	Moderately sorted	-0.10	Nearly symmetrical	1.30	Leptokurtic
	14	0.93	Coarse Sand	0.72	Moderately sorted	-0.09	Nearly symmetrical	1.01	Mesokurtic
	15	0.87	Coarse Sand	0.63	Moderately well sorted	-0.17	Coarse skewed	1.10	Mesokurtic
Middle Pleistocene	16	1.47	Medium Sand	1.13	Poorly sorted	-0.05	Nearly symmetrical	1.61	Very leptokurtic
	17	0.80	Coarse Sand	0.68	Moderately well sorted	0.11	Fine Skewed	1.01	Mesokurtic
	18	-0.13	V coarse Sand	0.44	Well sorted	1.00	Strongly fine skewed	0.94	Mesokurtic
	19	0.63	Coarse Sand	0.58	Moderately well sorted	0.12	Fine Skewed	1.49	Leptokurtic
	20	0.73	Coarse Sand	0.72	Moderately sorted	0.23	Fine Skewed	1.71	Very leptokurtic
	21	0.53	Coarse Sand	0.46	Well sorted	0.07	Nearly symmetrical	1.07	Mesokurtic
	22	0.77	Coarse Sand	0.62	Moderately well sorted	-0.03	Nearly symmetrical	0.94	Mesokurtic
	23	0.47	Coarse Sand	0.35	Well sorted	-0.07	Nearly symmetrical	1.04	Mesokurtic
	24	0.00	Coarse Sand	0.12	V well sorted	0.14	Fine Skewed	0.68	Platykurtic
	25	0.10	Coarse Sand	0.18	V well sorted	0.27	Fine Skewed	1.18	Leptokurtic
	26	0.13	Coarse Sand	0.17	V well sorted	0.12	Fine Skewed	1.09	Mesokurtic
	27	0.83	Coarse Sand	0.74	Moderately sorted	0.20	Fine Skewed	1.39	Leptokurtic
	28	-0.67	V coarse Sand	-0.10	V well sorted	1.00	Strongly fine skewed	2.05	Very leptokurtic
	29	0.30	Coarse Sand	0.26	V well sorted	-0.06	Nearly symmetrical	1.08	Mesokurtic
	30	0.60	Coarse Sand	0.51	Moderately well sorted	0.04	Nearly symmetrical	0.89	Platykurtic
	31	-0.20	V Coarse Sand	0.06	V well sorted	0.37	V fine skewed	1.07	Very leptokurtic
	32	-0.73	V Coarse Sand	-0.25	V well sorted	1.00	V fine skewed	1.89	Very leptokurtic
	33	-0.63	V Coarse Sand	-0.15	V well sorted	0.71	fine skewed	1.64	Very leptokurtic
34	0.93	Coarse Sand	0.82	Moderately sorted	0.15	Fine skewed	1.05	Mesokurtic	
35	-0.57	V coarse Sand	-0.06	V well sorted	0.88	V fine skewed	1.49	Leptokurtic	
36	0.17	Coarse Sand	0.20	V well sorted	0.04	Nearly symmetrical	1.18	Leptokurtic	
37	0.63	Coarse Sand	0.54	Moderately well sorted	0.10	fine skewed	1.17	Leptokurtic	
Late Plei.	38	0.37	Coarse Sand	0.44	Well sorted	0.18	Fine Skewed	0.92	Mesokurtic
	39	1.03	Medium Sand	0.86	Moderately sorted	0.10	Fine Skewed	1.02	Mesokurtic
	40	0.47	Coarse Sand	0.33	V well sorted	-0.10	Nearly symmetrical	1.28	Leptokurtic
Holocene	41	1.43	Medium Sand	1.09	Poorly sorted	-0.03	Nearly symmetrical	0.91	Mesokurtic
	42	1.60	Medium Sand	1.17	Poorly sorted	-0.15	Coarse skewed	0.96	Mesokurtic
	43	1.40	Medium Sand	1.05	Poorly sorted	-0.06	Nearly symmetrical	0.98	Mesokurtic
	44	1.43	Medium Sand	1.06	Poorly sorted	-0.12	Coarse skewed	1.04	Mesokurtic
	45	1.73	Medium Sand	1.24	Poorly sorted	-0.15	Coarse skewed	1.05	Mesokurtic
	46	1.07	Medium Sand	0.83	Moderately sorted	-0.05	Nearly symmetrical	1.17	Leptokurtic
	47	1.93	Medium Sand	1.55	Poorly sorted	0.02	Nearly symmetrical	1.20	Leptokurtic
	48	1.20	Medium Sand	0.95	Moderately sorted	-0.01	Nearly symmetrical	0.95	Mesokurtic
	49	1.00	Medium Sand	0.81	Moderately sorted	-0.08	Nearly symmetrical	0.53	Very platykurtic

The studied Pleistocene and Holocene sediments are identified to transported by two mode of transportation. The saltation population was considered the main population of transportation mechanism with small contributions from rolling populations (Fig. 4). The calculated grain size parameters (Folk and Ward, 1957) revealed that the studied sediments show significant variation in main size and sorting, in particular skewness and kurtosis (Fig. 5).

The presence of coarse-grained materials in the studied sediments indicated the high energy conditions that remove the small-sized sediments. The observed variation of the calculated grain size parameters and the dominance of rolling and saltation population confirmed their riverine and fluvial provenance and reveals sliding and saltation agents of the point bars of the braided channels (Mahmoud, 2018). The results of the grain size analysis indicate high energy current of braided channels.

Depositional environments, textural and mineralogical characteristics

Fig. 3: Plotting of the studied sediments on the ternary diagram proposed by Folk (1954).

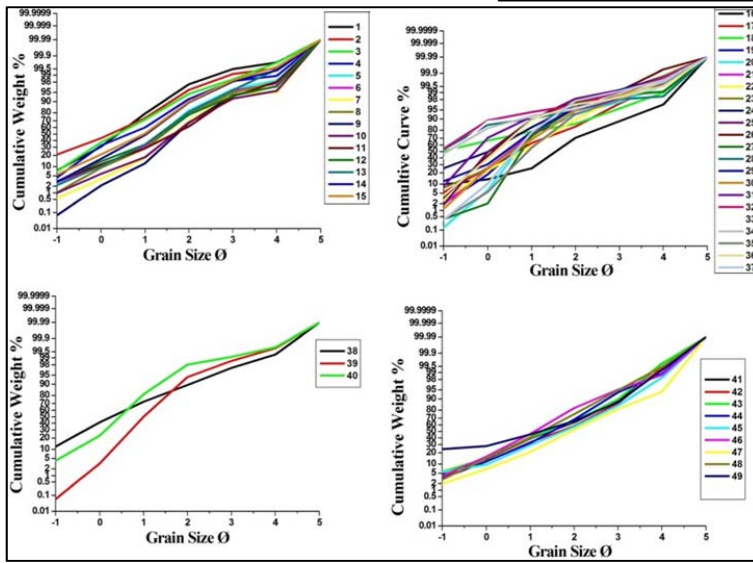
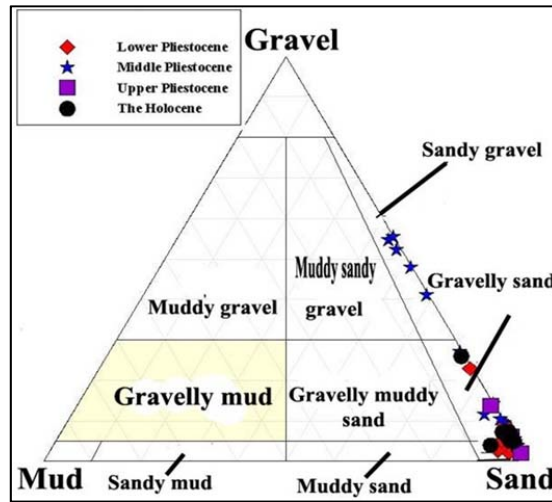
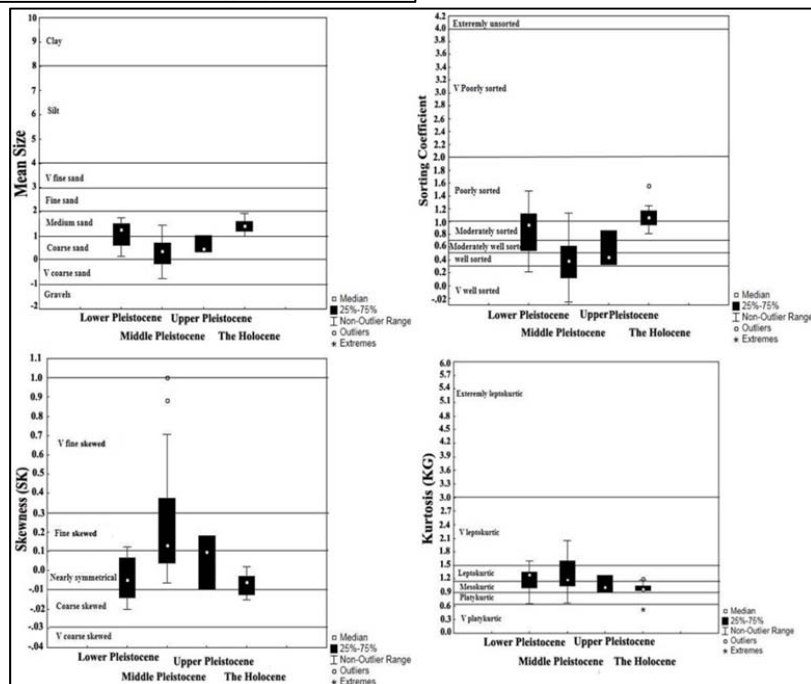


Fig. 4: Probability cumulative curves of the studied sediments samples

Fig. 5: Boxplots of mean size, sorting coefficient, skewness and kurtosis of the studied sediments.



Gravelmetric Analysis

The collected gravels are considered as pebbles size (i.e. 4 to 64 mm). Using Zingg Index (Zingg, 1935) the studied gravels can be classified as 55.8 % discoidal, 26.7 % spherical, 10.5 % rod-shape and 7 % bladed-shape (Fig. 6), which indicate that these gravels were transported mainly by water current. The investigated thin sections revealed that most of gravels are of sedimentary origin beside few igneous and metamorphic clasts (Fig 7).

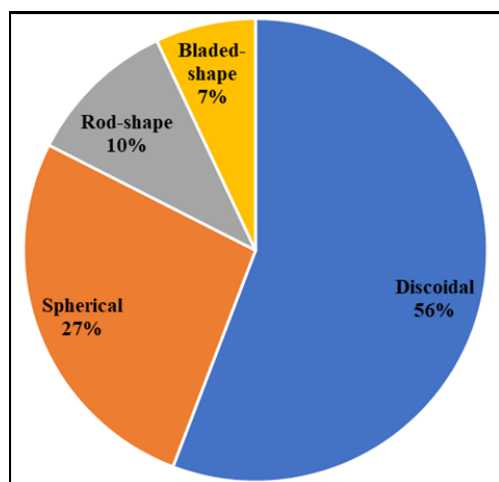
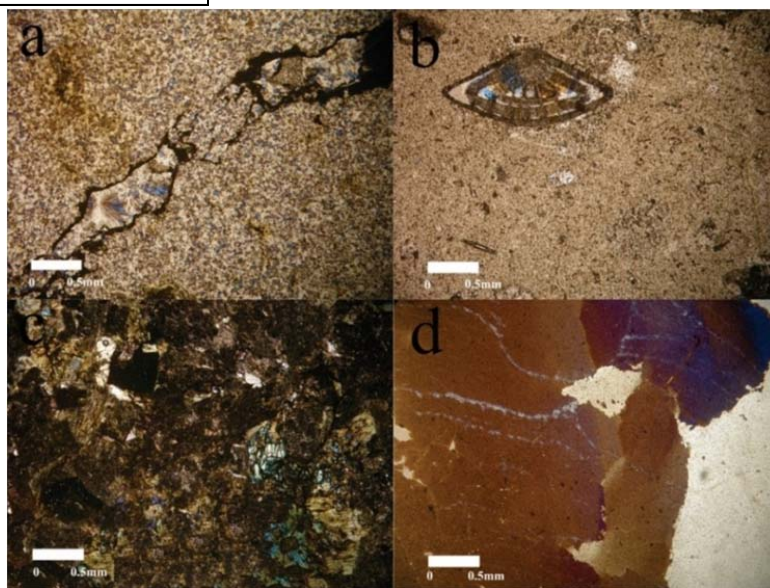


Fig. 6: Pie diagrams showing the different gravel shapes

Fig. 7: Photomicrographs showing different gravel compositions, (a) chert; (b) limestone; (c) altered volcanic rock; (d) deformed quartz in metamorphic rock



Mineralogy

The first part of the mineralogical analysis was carried out on some selected bulk samples using XRD technique. The data of bulk samples (Fig. 8) show that the essential silicate minerals are quartz, albite and illite (?), whereas non-silicate minerals include calcite and gypsum.

The percentage of the heavy index of the studied samples ranges between 1.57% and 18.68% (average 3.88%) and the percentage of the light index in the studied samples range between 81.32 to 98.43% (average 96.12 %). The light fraction of the samples under investigation is mainly composed of quartz grains (up to 98.00 %) with minor amount of altered feldspars. Both opaque and non-opaque heavy minerals constitute the heavy mineral assemblage of the studied sediment samples. The opaque minerals, which could not be segregated effectively in the present study, are mostly magnetite, ilmenite, hematite and limonite (Shukri, 1950; Hassan, 1976). The average percentage of these minerals constitute 62.29, 65.29, 64.31 and 55.91% of the total heavy population of Early Pleistocene, Middle Pleistocene, Late

Depositional environments, textural and mineralogical characteristics

Pleistocene and Holocene sediments; respectively (Table 4; Fig. 9). Non-opaque heavy mineral assemblages of the Pleistocene and Holocene in terms of mineral species are very similar. They consist of pyroxene, amphiboles, epidote, zircon, tourmaline, rutile, garnet, staurolite and kyanite. Andalusite, titanite and monazite are recorded in a few samples. In the present study they have been categorized as ultrastable, metastable and unstable.

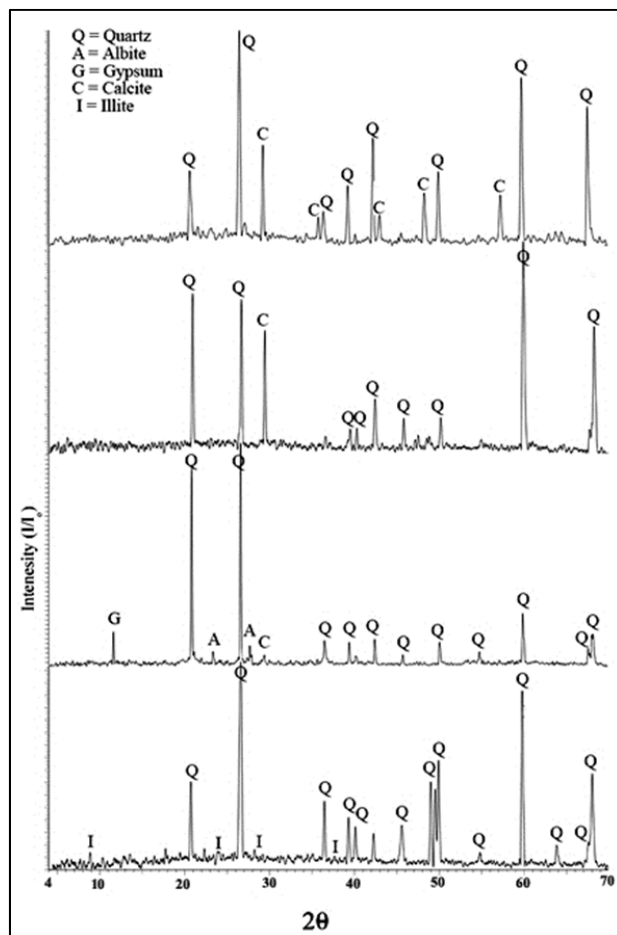


Fig. 8: X-ray diffractograms of bulk samples.

Ultrastable heavy minerals of the studied sediments include zircon, tourmaline, and rutile. Zircon is the most dominant mineral in this group. It occurs as colourless prismatic, rounded and subrounded grains. Some zircon grains are fractured and invariably contain inclusions (Fig. 10). The observed tourmaline grains have brown colour. They are strongly pleochroic prismatic and sub-rounded, sometimes are recorded as euhedral gains (Fig. 10). Rutile grains is characterised by deep red and reddish-brown colour, broad and thick boarder and short prismatic shape with subrounded corners (Fig. 10).

Unstable heavy minerals include amphiboles and pyroxenes. Amphibole group in the studied sediments is represented mainly by hornblende and tremolite. Hornblende is characterized by green color and distinct cleavage (Fig. 11). Pyroxenes are represented mainly by augite. The pyroxene grains vary between colorless to green in color, fresh to partially altered, subrounded to subangular, and show fractures and inclusions (Fig. 11). Owing to the unstable nature of amphibole and pyroxene their occurrence is usually limited to younger sediments (Pettijohn, 1941, 1975; Morton, 1985).

Metastable heavy minerals include epidote, garnet, staurolite and kyanite. The epidote grains are mainly prismatic with yellowish green color (Fig. 11). The garnet is mainly pale pink and sometimes colourless, these grains are rounded to subangular some of these grains are fractured. Most of the observed garnet grains contain inclusions in a few instances the grain surfaces are pitted (Fig. 11). Staurolite is found as subangular grains with yellowish brown and pale-yellow color, some grains contain inclusions (Fig. 11). The detected kyanite grains are colourless elongated cleavable prismatic grains (Fig. 11).

Table 4: Relative abundances of heavy minerals from the studied sediments

Age	S.No.	Op	Py	Am	Zrn	Tou	Rut	Ept	Gar	Sta	Ky	Others	ZTR
Early Pleistocene	1	59.59	8.72	4.36	3.20	3.49	0.87	13.95	2.91	1.45	0.87	0.58	23.42
	2	64.67	6.31	4.42	3.15	2.84	0.95	14.20	1.26	1.26	0.63	0.32	24.72
	3	65.35	6.08	5.17	2.74	3.95	1.52	10.94	0.30	2.74	0.91	0.30	31.40
	4	60.56	7.14	5.28	0.93	2.17	1.24	19.25	2.17	0.93	0.00	0.31	12.50
	5	60.98	9.15	5.18	2.74	3.05	1.52	13.11	2.44	1.83	0.00	0.00	23.08
	6	62.69	7.46	5.97	4.48	2.69	1.19	12.84	1.19	0.60	0.60	0.30	29.17
	7	60.90	8.33	5.77	2.56	2.24	0.32	16.35	1.28	0.64	0.96	0.64	15.38
	8	57.88	8.36	4.50	3.22	2.89	1.93	17.04	2.57	0.96	0.64	0.00	23.58
	9	53.68	9.20	4.91	2.45	3.07	1.23	22.09	1.23	1.53	0.61	0.00	17.05
	10	66.77	7.42	4.75	2.97	2.67	1.19	11.28	1.19	1.19	0.30	0.30	26.14
	11	67.07	6.71	5.49	2.74	3.35	1.52	11.28	0.61	0.61	0.61	0.00	30.12
	12	65.22	9.32	4.66	2.48	1.86	1.24	11.80	1.55	0.93	0.62	0.31	19.35
	13	62.89	8.18	3.77	2.83	2.52	2.20	13.52	2.20	0.63	0.63	0.63	26.09
	14	61.54	9.23	3.38	3.08	2.77	1.54	15.08	2.46	0.92	0.00	0.00	23.76
	15	64.63	8.04	3.86	1.61	1.93	1.61	16.40	1.29	0.32	0.32	0.00	17.02
Ave.	62.29	7.98	4.76	2.75	2.77	1.34	14.61	1.64	1.10	0.51	0.25	22.85	
Middle Pleistocene	16	62.15	2.76	6.63	8.29	5.25	1.38	11.05	1.10	0.28	0.55	0.55	66.67
	17	48.54	6.07	9.71	7.28	7.04	1.21	17.96	0.73	0.73	0.49	0.24	43.54
	18	65.90	4.30	7.45	4.87	2.29	2.58	10.89	0.29	0.57	0.29	0.57	40.96
	19	78.53	4.19	3.40	1.83	1.57	0.79	8.64	0.52	0.26	0.26	0.00	24.24
	21	83.09	2.97	3.26	0.59	0.89	0.59	6.53	0.89	0.59	0.30	0.30	14.29
	22	66.27	7.83	3.92	3.31	2.11	1.51	12.95	0.90	0.90	0.30	0.00	25.84
	23	78.37	4.70	2.82	2.51	0.94	1.25	8.15	1.25	0.00	0.00	0.00	27.78
	24	75.53	7.55	3.32	1.21	0.60	0.00	10.88	0.30	0.00	0.60	0.00	8.00
	25	77.13	7.98	2.39	1.33	1.06	0.53	8.78	0.80	0.00	0.00	0.00	14.67
	26	67.28	6.12	5.50	2.75	2.14	0.61	13.46	0.92	0.61	0.00	0.61	20.69
	27	53.41	7.42	5.93	4.45	3.56	0.89	21.07	1.19	1.48	0.30	0.30	23.81
	28	81.33	3.01	3.31	2.11	1.20	0.00	6.63	1.20	1.20	0.00	0.00	21.57
	29	58.21	8.96	3.28	2.39	2.09	0.60	22.99	0.90	0.60	0.00	0.00	13.82
	30	55.73	9.91	3.72	3.10	2.79	0.93	22.29	0.93	0.31	0.31	0.00	18.18
	31	67.70	6.18	3.65	4.21	1.40	1.97	12.64	0.56	0.56	0.56	0.56	31.40
	32	56.98	9.97	3.42	3.42	3.13	1.42	18.52	1.42	0.00	0.85	0.85	23.33
	33	56.63	9.06	3.56	4.53	2.59	1.29	20.39	1.29	0.00	0.65	0.00	24.07
	34	57.14	7.43	4.29	4.29	1.43	0.57	21.43	1.43	0.57	1.14	0.29	17.32
35	56.71	9.15	3.66	3.66	1.83	1.22	20.12	1.83	0.91	0.91	0.00	18.33	
36	60.25	6.62	5.05	5.05	3.15	0.95	17.35	0.63	0.63	0.00	0.32	30.21	
37	64.31	9.54	3.27	1.91	0.82	1.09	16.62	0.27	1.09	0.54	0.54	12.17	
Ave.	65.29	6.75	4.36	3.48	2.28	1.02	14.73	0.92	0.54	0.38	0.24	24.80	
Late Pleic.	38	56.73	9.46	3.15	2.87	2.29	1.72	20.06	0.29	0.57	2.58	0.29	19.05
	39	65.77	6.85	3.57	2.68	1.49	1.19	13.69	2.38	2.08	0.00	0.30	18.75
	40	70.43	5.65	2.96	2.96	1.08	0.81	14.25	0.81	0.81	0.00	0.27	19.78
	Ave.	64.31	7.32	3.23	2.83	1.62	1.24	16.00	1.16	1.15	0.86	0.28	19.19
Holocene	41	57.36	15.71	5.74	3.24	2.99	1.25	11.22	1.75	0.50	0.25	0.00	21.28
	42	62.94	15.38	2.80	3.26	2.80	1.40	10.02	0.70	0.23	0.23	0.23	25.40
	43	63.19	17.31	3.02	2.20	1.92	1.10	9.62	1.10	0.27	0.27	0.00	16.52
	44	55.71	17.66	3.80	4.08	3.26	1.63	11.96	0.82	0.27	0.82	0.00	25.38
	45	62.64	15.66	3.36	2.24	2.01	0.89	11.41	0.89	0.45	0.45	0.00	15.97
	46	52.14	17.65	3.48	5.08	4.55	1.60	13.90	0.53	0.53	0.27	0.27	30.88
	47	47.83	17.39	1.45	8.99	4.64	2.32	13.91	1.74	1.45	0.00	0.29	44.35
	48	49.86	19.94	1.42	5.13	4.84	1.71	14.81	0.85	0.57	0.85	0.00	30.37
	49	51.55	16.75	1.55	6.44	4.64	1.80	13.66	1.55	1.55	0.52	0.00	36.23
	Ave.	55.91	17.05	2.96	4.52	3.52	1.52	12.28	1.10	0.65	0.41	0.09	27.38

Py= Pyroxene, Am= Amphiboles, Ru= Rutile, St= Staurolite, Ga= Garnet, Ep= Epidote, Tou= Tourmaline, Ky= Kyanite, Zrn= Zircon, Others= Sillimanite + Andalusite + Titanite, Op= Opaque.

Depositional environments, textural and mineralogical characteristics

Fig. 9: Pie diagrams showing the average percentage frequency distribution of the heavy minerals in the Pleistocene and the Holocene sediments.

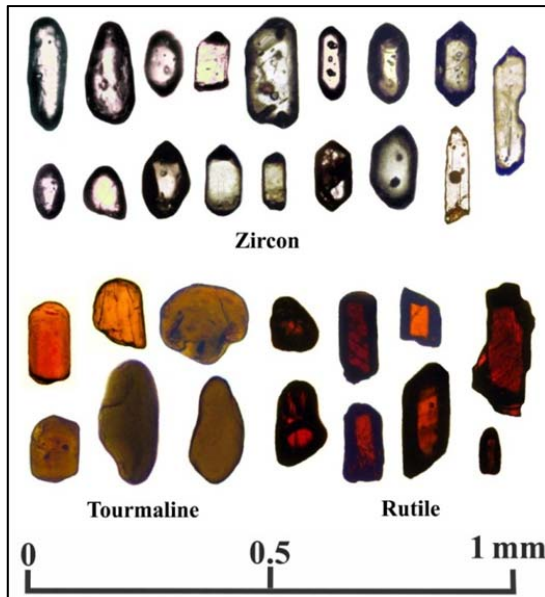
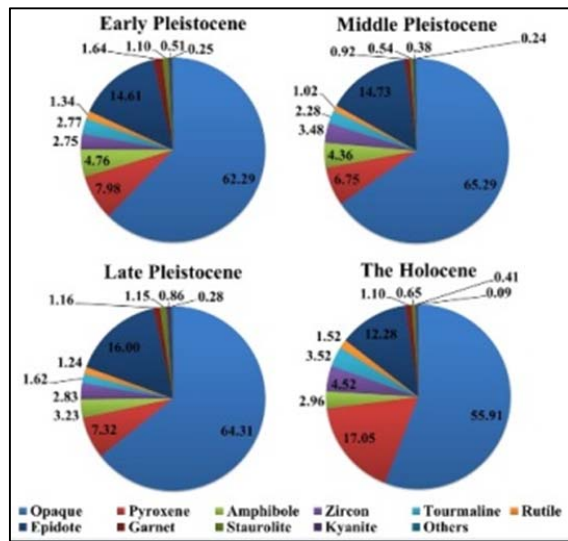
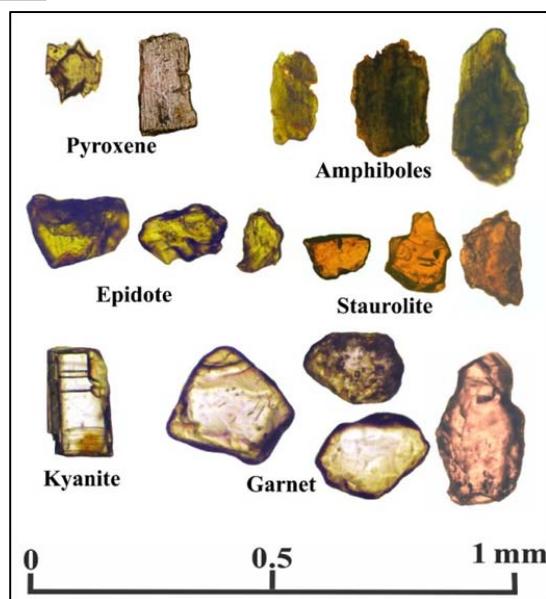


Fig. 10: Photomicrographs of ultrastable heavy minerals

Fig. 11: Photomicrographs of unstable and metastable heavy minerals



The mineralogical "maturity" of heavy mineral assemblages is quantitatively defined by zircon-tourmaline-rutile (ZTR; Hubert, 1962) index. The ZTR index is the percentage of the combined zircon, tourmaline, and rutile grains among the transparent, non-micaceous, detrital heavy minerals. As the ZTR index increases, concentration of the varieties of zircon, tourmaline, and rutile occurs, together with a decrease in the number of species of transparent heavy minerals. The ZTR index increases markedly even in mineralogically immature sediments. The ZTR index in respect of Pleistocene and Holocene sediments has been found to be 22.85, 24.80, 19.19 and 27.38 % for Early Pleistocene, Middle Pleistocene, Late Pleistocene and Holocene; respectively, suggesting mineralogically an overall immature nature.

Provenance

The textural and mineralogical data show some broad spatial patterns. The most prominent signals arise from textural attributes of these sediments are these sediments were deposited in fluvial environment confirmed the nature of cumulative curves. Generally, the grain-size characteristics of the Pleistocene and Holocene sediments accompanied with field observed sedimentary structures strongly suggest deposition under medium to high energy current of braided river.

The heavy minerals assemblage of the Pleistocene and Holocene sediments is by and large similar that suggest similar composition of the provenance throughout their sedimentation. In a synoptic view, this assemblage indicates a variety of probable source rock types including metamorphic, igneous, and sedimentary. In general, the heavy minerals show slight roundness, and, in many cases, they occur as angular to subangular grains.

The enrichment of pyroxenes and amphiboles in most of the studied samples show the role of basement rocks in their distribution. The presence of prismatic and rounded grains of ultra-stable minerals confirms the tow source of these sediments. High proportion of pyroxene resulted from erosion of Ethiopian volcanic terrains (Foucault and Stanley, 1989) and may be from nearby Oligocene basalt sheets. The metamorphic source is indicated by existence of epidote, garnet, kyanite, staurolite and andalusite (Milner et al. 1962).

CONCLUSIONS

The quantitative and qualitative determinations of the sedimentary structure and the grain size analysis of the Quaternary sediments in Kafr El Gebel area are measured. Most of them are a large scale planar wedged shape cross bedding coarse to very coarse sand grains transported by traction and saltation agents that indicate a medium to high energy current of the defunct network braided Nile channels. Non-opaque heavy mineral assemblages of the Pleistocene and Holocene in terms of mineral species are very similar. These are pyroxene, amphiboles, epidote, zircon, tourmaline, rutile, garnet, staurolite and kyanite. Andalusite, titanite and monazite are recorded in a few samples. The low values of ZTR index suggesting mineralogically immature nature of these sediments. The heavy minerals assemblage of these sediments indicates a variety of probable source rock types including metamorphic, igneous, and sedimentary.

REFERENCES

- Abuodha, J. O. (2003): Grain size distribution and composition of modern dune and beach sediments, Malindi Bay coast, Kenya. *J. Afr. Earth Sci.* 36:41-54.
- Alharbi, O. A., Williams, A. T., Phillips, M. R., Thomas, T. (2016): Textural characteristics of sediments along the southern Red Sea coastal areas, Saudi Arabia. *Arab. J. Geosci.* 9: 735.
- Butzer, K. W., Hansen, C. L. (1968): *Desert and River in Nubia: Geomorphology and Prehistoric Environments at the Aswan Reservoir.* University of Wisconsin Press, Madison, Wisconsin, 562 p.
- Craig, T., Jackson, J., Priestley, K., McKenzie, D. (2011): Earthquake distribution pat-terns in Africa: their relationship to variations in lithospheric and geological structure, and their rheological implications. *Geophys. J. Int.* 185: 403-434.
- Dawood, Y. H., Abd El Naby, H. H. (2012): Distribution of uranium and thorium radioelements in subsurface Pleistocene-Holocene sediments of the Nile Delta, Egypt. *JAKU Earth Sci.*, 23(2):149-168.
- de Heinzelin, J. (1968): Geological history of the Nile Valley in nubia. In: Wendorf, F. (Ed.), *The Prehistory of Nubia.* Southern Methodist University Press, 19-55.

Depositional environments, textural and mineralogical characteristics

- Dolson, J. C., Shann, M. V., Matbouly, S., Harwood, C., Rashed, R., Hammouda, H. (2001): The petroleum potential of Egypt. In: AAPG Memoir, 74. Chapter 23.
- Fielding, L., Najman, Y., Millar, I., Butterworth, P., Garzanti, E., Vezzoli, G., Barfod, D., Kneller, B. (2018) The initiation and evolution of the River Nile. *Earth Planet. Sci. Lett.* 489:166-178.
- Folk, R. L. (1954): The distinction between grain size and mineral composition in sedimentary nomenclature. *J. Geol.* 6(4):344-359.
- Folk, R. L. (1966): A review of grain size parameters. *Sedimentology* 6:73-93.
- Folk, R. L., Ward, W. C. (1957): Brazos River bar- a study in the significance of grain size parameters. *J. Sed. Petrol.* 27(1):3-26.
- Foucault, A., Stanley, D. J. (1989): Late Quaternary palaeoclimatic oscillations in East Africa recorded by heavy minerals in the Nile delta. *Nature* 339:44-46.
- Friedman, G. M. (1961): Distinction between dune, beach and river sand from their textural characteristics. *J. Sed. Petrol.* 31(4): 514-529.
- Frihy, O. E., Lotfy, M. F. Komar, P. D. (1995): Spatial variations in heavy minerals and patterns of sediment sorting along the Nile Delta, Egypt. *Sediment. Geol.* 97: 33-41.
- Galehouse, J. S. (1971): Point counting. In: Carver, R.E. (ed) *Procedures in sedimentary petrology*. Jhon Wiley intersciences, New York, 385-407.
- Garzanti, E., Andò, S., and Vezzoli, G. (2009): Grain-size dependence of sediment composition and environmental bias in provenance studies. *Earth Planet. Sci. Lett.* 277: 422-432.
- Garzanti, E., Andò, S., Limonta, M., Fielding, L., Najman, Y. (2019): Diagenetic control on mineralogical suites in sand, silt, and mud (Cenozoic Nile Delta): Implications for provenance reconstructions. *Earth-Sci. Rev.* 185:122-139.
- Garzanti, E., Andò, S., Padoan, M., Vezzoli, G., El Kammar, A. (2015): The modern Nile sediment system: processes and products. *Quat. Sci. Rev.* 130: 9-56.
- Garzanti, E., Andò, S., Vezzoli, G., Ali Abdel Megid, A., El Kammar, A. (2006): Petrology of Nile River sands (Ethiopia and Sudan): sediment budgets and erosion patterns. *Earth Planet. Sci. Lett.* 252:327-341.
- Giorgetti, G., Talarico, F., Sandroni, S. and Zeoli, A. (2009): Provenance of Pleistocene sediments in the ANDRILL AND-1B drillcore: Clay and heavy mineral data. *Glob. Planet. Change* 69:94-102.
- Hamdan, M. A., Hassan, F. A., Flower, R. J., Leroy, S. G., Shallaly, N. A., Flynn, A. (2019): Source of Nile sediments in the floodplain at Saqqara inferred from mineralogical, geochemical, and pollen data, and their palaeoclimatic and geochronological significance. *Quat. Int.* 501:272-288.
- Hassan, F. A. (1976): Heavy Minerals and the Evolution of the Modern Nile. *Quat. Res.* 6:425-444.
- Hubert, J. F. (1962): A zircon-tourmaline-rutile maturity index and the interdependence of the composition of heavy mineral assemblages with the gross composition and texture of sandstones. *J. Sed. Petrol.* 32: 440-450.
- Johnsson, M. J. (1993): The system controlling the composition of clastic sediments. In: Johnsson MJ, Basu A (Eds.), *Processes Controlling the Composition of Clastic Sediments*. Geological Society of America, Special Paper 284: 1-19.
- Johnsson, M. J., Meade, R. H. (1990): Chemical weathering of fluvial sediments during alluvial storage: the Macuapanim Island point bar, Solimoes River, Brazil. *J. Sed. Petrol.* 60:827-842.
- Kasper-Zubillaga, J. J., Carranza-Edwards, A. and Morton-Bermea, A. (2008): Heavy minerals and rare earth elements in coastal and inland dune sands of El Vizcaino Desert, Baja California Peninsula, Mexico. *Mar. Geores. Geotechnol.* 26(3):172-188.
- Lahijani, H. and Tavakoli, V. (2012): Identifying provenance of South Caspian coastal sediments using mineral distribution pattern. *Quat. Int.* 261:128-137.
- Lario, J., Spencer, C., Plater, A. J., Zazo, C., Goy, J. L., Dabrio, C. J. (2002): Particle size characterisation of Holocene back-barrier sequences from North Atlantic coasts (SW Spain and SE England). *Geomorphology*, 42: 25-42.
- Macgregor, D. S. (2012): The development of the Nile drainage system: integration of onshore and offshore evidence. *Pet. Geosci.*, 18: 417-431.
- Mahmoud, A. A. (2018) A guide to the Egyptian sediments, Latvia, European Union, ppt.194.

- Mahmoud, A. A. and Hamdan, M. A. (2002): On the stratigraphy and lithofacies of the Pleistocene sediments at Giza Pyramidal area, Cairo, Egypt, *Sedimentology of Egypt* 10:145-158.
- Mange, M. A. and Maurer, H. W. (1992): *Heavy Minerals in Colour*. Chapman Hall, London, UK. 147p.
- Milner, H. B., Ward, A. M. and Highan, F. (1962): *Sedimentary petrography*, v.11, principle and application. 4th ed. New York: The Macmillan.
- Morton, A. C. (1985): Heavy minerals in provenance studies. In: *Provenance of arenites*, G.G., Zuffa (Ed.), Dordrecht, Reidel, 249-77.
- Morton, A. C. and Hallsworth, C. (1994): Identifying provenance-specific features of detrital heavy mineral assemblages in sandstones. *Sediment. Geol.* 90 (3,4):241-256.
- Mycielska-Dowgiało, E. and Ludwikowska-Kędzia M. (2011): Alternative interpretations of grain-size data from quaternary deposits. *Geologos* 17(4):189-203.
- Nechaev, V. P. and Ispording, W. C. (1993): Heavy-mineral assemblages of continental margins as indicators of plate-tectonic environments. *J. Sed. Petrol.* 63: 1110-1117.
- Omara, S. (1952): The structural features of the Giza Pyramids area. Unpublished Ph. D. Thesis, Fac. Sci. Cairo Univ. 85p.
- Pettijohn F. J. (1941): Persistence of heavy minerals and geologic age. *J. Geol.* 49:610-625.
- Pettijohn F. J. (1975): *Sedimentary rocks*. 3rd Edition, Harper & Row Publ., 628 p.
- Said, R. (1962): *The Geology of Egypt*: Elsevier Publ. Co.
- Said, R. (1975): *Subsurface geology of Cairo area*, Memoires de L'Institut d'Egypte, tome soixante, Cairo.
- Said, R. (1993): *The River Nile: Geology, Hydrology and Utilization*. Pegamon Press, Oxford, 320 p.
- Said, R. (1981): *The Geological Evolution of the River Nile*. Springer-Verlag Inc, New York, 151 p.
- Salem, R. (1976): Evolution of Eocene–Miocene sedimentation patterns in parts of Northern Egypt. *AAPG Bull.* 60:34-64.
- Savage, K. M. and Potter, P. E. (1991): Petrology of modern sands of the Rios Guaviare and Inirida, southern Colombia: tropical climate and sand composition. *J. Geol.* 99:289-298.
- Sawakuchi, A. O., Giannini, P. F., Martinho, C. T. and Tanaka, A. B. (2009): Grain size and heavy minerals of the Late Quaternary eolian sediments from the Imbituba–Jaguaruna coast, Southern Brazil: Depositional controls linked to relative sea-level changes. *Sediment. Geol.* 222: 226-240.
- Sharafeldin, S. M., Essa, K. S., Youssef, M. A. S., Karsli, H. and Diab, Z. E., Sayil, N. (2019): Shallow geophysical techniques to investigate the groundwater table at the Great Pyramids of Giza, Egypt. *Geoscientific Instrumentation Methods and Data Systems*, 8: 29-43.
- Shukri, N. M. (1950): The mineralogy of some Nile sediments. *Quart. Jour. Geol. Soc. London*, 105:511-534.
- Shukri, N. M. (1951): Mineral analysis table of some Nile sediments. *Bull. Inst. De Desert, Cairo*, 1:39-67.
- Siegel, F. R., Gupta, N., Shergill, B., Stanley, D. J. and Gerber, C. (1995): Geochemistry of Holocene sediments from the Nile delta. *J. Coast. Res.* 11(2):415-431.
- Stanley, D. J. and Wingerath, J. G. (1996): Clay mineral distributions to interpret Nile Cell provenance and dispersal: I. Lower River Nile to Delta sector. *J. Coast. Res.* 12:911-929.
- Strougo, A. (1979): The Middle Eocene-Upper Eocene boundary in Egypt. *Ann. Geol. Surv. Egypt*, IX: 455-470.
- Strougo, A. (1985): Eocene stratigraphy of the Giza Pyramid Plateau. *M.E.R.C. Ain Shams Univ., Earth Sci. Res. Ser.* 5:79-99.
- Underwood, C. J., King, C., and Steurbaut, E. (2013): Eocene initiation of Nile drainage due to East African uplift. *Palaeogeogr. Palaeoclimatol. Palaeoecol.* 392:138-145.
- von Eynatten, H. and Dunkl, I. (2012): Assessing the sediment factory: The role of single grain analysis. *Earth-Sci. Rev.* 115: 97-120.
- Weltje, G. J., and von Eynatten, H. (2004): Quantitative provenance analysis of sediments: review and outlook. *Sediment. Geol.* 171: 1-11.
- Wendorf, F. and Schild, R. (1976): *Prehistory of the Nile Valley*. Academic Press, London, 404 p.
- Wong, F. L. (2002): Heavy mineral provinces of Palos Verdes margin, southern California. *Cont. Shelf Res.* 22: 899-910.

البيئات الترسيبية، الخصائص النسيجية والمعدنية لرواسب العصر الرباعي المنكشفة، الجيزة ، مصر

أمينة السيد^١، عبد المنعم محمود^١، أحمد جاد^٢، أميرة خطاب^١

^١ قسم العلوم البيولوجية والحيولوجية، كلية التربية، جامعة عين شمس، القاهرة، مصر

^٢ قسم الجيولوجيا، كلية العلوم، جامعة عين شمس، القاهرة، مصر

الخلاصة

تظهر مكاشف رواسب العصر الرباعي على نطاق واسع في منطقة كفر الجبل ، الواقعة في الجيزة ، مصر . تمت دراسة عشرة قطاعات استراتيجرافية وجمع واحد وخمسين عينة منها لدراسة خصائصها النسيجية والمعدنية بغرض تحديد التاريخ الرسوبي للصخور . أظهرت المعاملات الإحصائية لحجم الحبيبات أن الرواسب يهيمن عليها رمل يتميز أساساً بكونه متوسط إلى خشن ، وذو فرز رديء إلى جيد جداً ، ولهذه الرواسب منحنيات التواء شبه متماثلة ذات تفلطح متوسط إلى مدبب . من الناحية المعدنية تتكون المعادن الخفيفة بهذه الرواسب من الكوارتز مع كمية قليلة من الفلسبار . يسود مجموعة المعادن الثقيلة غير المعتمدة كل من البيروكسين والأمفيبول والإبيدوت والزركون والتورمالين والروتيل والجارنت والستوروليت والكيانيت. بالإضافة إلى ذلك، تم التعرف على الأندليوسيت والتيتانيت والمونازيت في بعض العينات . تشير الخصائص النسيجية والمعدنية لرواسب العصر الرباعي إلى عدم النضج المعدني. وقد نشأت هذه الرواسب من مجموعة متنوعة من الصخور المصدر المتحولة، والنارية والرسوبية. تم نقل نواتج تجوية هذه الصخور عن طريق الأنهار والجداول وتراكمت في أنواع مختلفة من البيئات النهرية .